International Journal of Heat and Mass Transfer 102 (2016) 264–276

Contents lists available at ScienceDirect

International Journal of Heat and Mass Transfer

journal homepage: www.elsevier.com/locate/ijhmt

Systematic measurements of heat transfer characteristics in saturated pool boiling of water-based nanofluids

Muhamad Zuhairi Sulaiman [a,b], Daisuke Matsuo [a], Koji Enoki [a], Tomio Okawa [a,*]

[a] Department of Mechanical and Intelligent Systems, The University of Electro-Communications, 1-5-1, Chofugaoka, Chofu-shi, Tokyo 182-8585, Japan
[b] Faculty of Mechanical Engineering, Universiti Malaysia Pahang, 26600 Pekan, Malaysia

ARTICLE INFO

Article history:
Received 5 January 2016
Received in revised form 9 May 2016
Accepted 6 June 2016

Keywords:
Nanofluid
Saturated pool boiling
Particle material
Particle concentration
Particle dispersion condition
Heat transfer coefficient
Critical heat flux

ABSTRACT

Experiments were carried out to investigate the heat transfer characteristics in saturated pool boiling of water-based nanofluids. An upward-facing copper surface of 20 mm in diameter was used as the heated surface. Main experimental parameters in this work were nanoparticles' material (TiO_2, Al_2O_3 and SiO_2), mass concentration (0.04, 0.4 and 1 kg/m^3) and dispersion condition (fine and coarse dispersions). Effects of these parameters on the time-variation of wall superheat under constant heat flux, the heat transfer coefficient (boiling curve) and the critical heat flux (CHF) were explored. It was found that the particle dispersion condition has no noticeable influence on the heat transfer characteristics within the range tested in this work. Whilst, the material and concentration of nanoparticles greatly affected the time-variation of wall superheat and the boiling curve. In particular, it was found that the wall superheat likely to increase significantly when the nanoparticle layer formed on the heated surface is partially detached. The CHF in nanofluid was 2.5–3 times higher than that for pure water in all the experimental conditions.

1. Introduction

Since You et al. reported considerable CHF enhancement up to 200% in saturated pool boiling of Al_2O_3–water nanofluids [1], many experimental works have been conducted for the boiling heat transfer of nanofluids [2–8]. These studies revealed the effects of several important parameters on the boiling heat transfer characteristics. For instance, Kim extensively surveyed the experimental results reported in literature to show that the critical heat flux (CHF) enhancement in water-based nanofluids tends to be less significant with increased values of the heater size and pressure [3]. However, the effects of other parameters including the material and size of nanoparticles on the CHF have not been understood sufficiently.

During the nucleate boiling of nanofluids, nanoparticles are deposited on the heated surface to alter the surface properties such as the wettability, roughness and capillarity [9–15]. It was found that the CHF is usually enhanced in nanofluids mainly due to the modification of the heated surface properties [16–20]. The nucleate boiling heat transfer in nanofluids is however more complicated. It may be enhanced, deteriorated, or stay unchanged depending on the experimental conditions [21–25]. In particular, Barber et al. [5] pointed out that the experimental results of the boiling heat transfer of nanofluids reported in literature are inconsistent even under similar experimental conditions. The complex time-variation of the boiling heat transfer in nanofluid would be one of the main reasons of such inconsistency [19]. No systematic experimental information is however available in literature for the boiling heat transfer in nanofluids.

As is widely-known, boiling heat transfer characteristics is of significant practical importance in a variety of industrial applications including heat exchangers, cooling of high-power-density electronic devises, quench hardening of steel and cast iron alloys, and emergency cooling of nuclear power plants. The use of nanofluid as the coolant is one of the promising methods to further enhance the boiling heat transfer characteristics since the significant increase of CHF is achieved even at low nanoparticle concentrations. However, sufficient experimental information is necessary to use the nanofluids in the above-mentioned applications.

The main objective of this work is to provide systematic experimental information on the effects of nanoparticles' material, concentration and dispersion condition on the heat transfer characteristics of nucleate pool boiling in water-based nanofluids. Other important parameters are set to the values that are considered as standard; namely, the experiments are performed under the atmospheric pressure and the bulk liquid was kept at

* Corresponding author. Tel.: +81 42 443 5404; fax: +81 42 484 3327.
E-mail address: okawa.tomio@uec.ac.jp (T. Okawa).

http://dx.doi.org/10.1016/j.ijheatmasstransfer.2016.06.017
0017-9310/

Nomenclature

C	nanoparticle concentration (kg/m^3)
d_p	primary particle diameter (m)
d_{sm}	Sauter mean diameter (m)
t_{us}	excitation time in ultrasonic bath (s)
q_{CHF}	critical heat flux (W m^{-2})
q_W	heat flux (W m^{-2})
t_b	boiling time (s)
Q	heater power (W)
T_1	copper block temperature (K)
Greek symbols	
ΔT_{BW}	bottom wall superheat (K)
ΔT_W	wall superheat (K)
θ	contact angle (degree)

the saturation temperature. The upward-facing copper surface of 20 mm in diameter is used as the heated surface.

2. Experimental methods

2.1. Experimental apparatus

The schematic diagram and photo of the experimental apparatus are presented in Fig. 1(a) and (b), respectively. The test vessel consisted of a polycarbonate circular tube used as a side wall, a stainless steel bottom plate and a polycarbonate top plate. The inner diameter and the height of the vessel were 144 and 170 mm, respectively, and the side wall of the vessel was covered with the thermal insulator. The heating device was mounted concentrically at the bottom of the test vessel. The one end of a copper block was machined into a cylindrical shape of 20 mm diameter. Its end face was used as the heated surface. Nine cartridge heaters rated at 900 W in total were embedded in the other end of the copper block; the maximum heat flux is hence calculated to be 2.86 MW/m^2. Four type-K thermocouples accurate to within ±1.5 K were positioned along the central axis of the copper cylinder to measure the heat flux q_W and the wall superheat ΔT_W and to shut down the system when the critical heat flux condition was reached. Using the uncertainty analysis method described by Cooke and Kandlikar [26], the measurement uncertainties of q_W and ΔT_W were estimated within less than 90 kW/m^2 and 3 K, respectively. As delineated in Fig. 1(a), the copper block was put in the stainless steel jacket of 2 mm in thickness to reduce the heat loss from the side wall of the block. The copper block and the jacket were bonded smoothly by means of electron-beam welding not only to avoid leakage but to eliminate significant vapor bubble generation at the bond part. An immersion heater of 1 kW was arranged in the lower part of the vessel to keep the bulk liquid temperature at the saturation temperature. A reflux condenser cooled with tap water was equipped on the top plate to prevent the vapor release from the test vessel. Since the top of the condenser was open to the atmosphere, the pressure inside the vessel was assumed equal to the atmospheric pressure. A type-K thermocouple was positioned 10 mm above the center of the heated surface to confirm that the bulk liquid was in the saturation condition. The top plate had a 15 mm diameter hole to inject the nanofluid into boiling water in the vessel using a syringe; the hole was closed with a silicone rubber plug except during the nanofluid injection.

2.2. Preparation of nanofluids

The following three types of nanoparticles of white color manufactured by Aerosil Corporation were used to prepare the nanofluids: (1) Aeroxide TiO_2 P 25 (TiO_2 particles that are the mixture of anatase (80%) and rutile (20%) crystal structures with the average

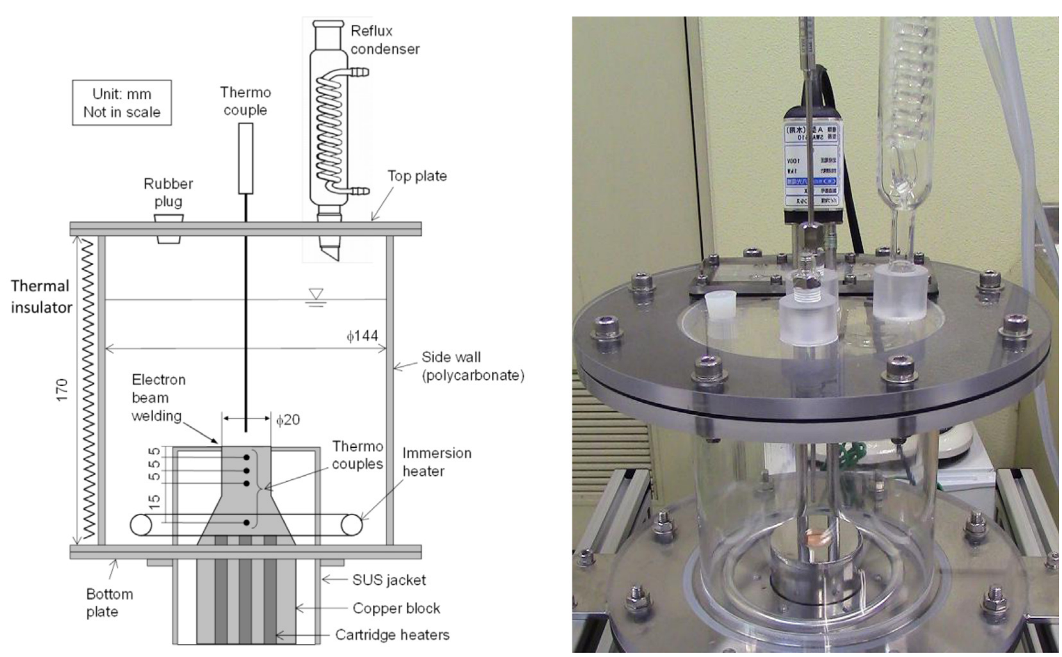

(a) Schematic diagram (b) Photo

Fig. 1. Experimental apparatus.